Optimization of the time-dependent traveling salesman problem with Monte Carlo methods

Johannes Bentner,* Günter Bauer, Gustav M. Obermair, and Ingo Morgenstern
Fakultät Physik, Universität Regensburg, D-93040 Regensburg, Germany

Johannes Schneider
Physik-Institut, Universität Zürich-Irchel, Winterthurerstrasse 190, CH-8057 Zürich, Switzerland
(Received 5 January 2001; published 8 August 2001)

A problem often considered in operations research and computational physics is the traveling salesman problem, in which a traveling salesperson has to find the shortest closed tour between a certain set of cities. This problem has been extended to more realistic scenarios, e.g., the ''real'' traveling salesperson has to take rush hours into consideration. We will show how this extended problem is treated with physical optimization algorithms. We will present results for a specific instance of Reinelt's library TSPLIB95, in which we define a zone with traffic jams in the afternoon.

DOI: 10.1103/PhysRevE.64.036701 PACS number(s): 02.70.Uu, 05.10.Ln, 02.50.Ng, 02.50.Ga

I. INTRODUCTION

A. Physical optimization algorithms

For many years, physical optimization algorithms have been used in physics to find the global optimum or at least a quasioptimum state of a complex system that cannot be solved analytically in simulations on a computer. These algorithms use an annealing technique, which is motivated from solid state physics: by lowering the temperature T successively, the system loses energy to a large extent and is therefore transferred from a highly energetic unordered configuration to an ordered solution of low energy. At each temperature, a certain number of changes within the configuration (called moves) are performed. The choice of the moves is performed randomly, which is why this class of algorithms is part of Monte Carlo simulations.

Usually, two assumptions are made for the system to be optimized and for the simulated annealing (SA) algorithm.

(1) The system should be classical, i.e., it should obey Boltzmann statistics: the probability $\pi(\sigma)$ of a configuration σ is given by

$$\pi(\sigma)=\frac{1}{Z}\exp\left(-\frac{\mathcal{H}(\sigma)}{k_BT}\right) \tag{1}$$

with the energy $\mathcal{H}(\sigma)$ of the configuration σ, the temperature T, the Boltzmann factor k_B, and the partition function

$$Z=\sum_{\tau}\exp\left(-\frac{\mathcal{H}(\tau)}{k_BT}\right). \tag{2}$$

k_B will be set to 1 throughout this paper and the energy and the temperature will be considered to be dimensionless.

(2) The system should be brought to a state of equilibrium at each temperature by a series of move trials for which the optimization algorithm has to provide an appropriate acceptance criterion. A suitable condition for this is detailed balance [1],

$$\pi(\sigma)p(\sigma\rightarrow\tau)=\pi(\tau)p(\tau\rightarrow\sigma), \tag{3}$$

i.e., the relation of the transition probabilities p between σ and τ is given by the ratio of the probabilities $\pi(\sigma)$ and $\pi(\tau)$.

However, some arbitrariness in the explicit choice of the transition probability remains. In most cases the Metropolis criterion [2] is used, so that a move is accepted according to

$$p(\sigma\rightarrow\tau)=\begin{cases}\exp\left(-\dfrac{\Delta\mathcal{H}}{T}\right) & \text{if } \Delta\mathcal{H}>0\\ 1 & \text{otherwise}\end{cases} \tag{4}$$

with $\Delta\mathcal{H}=\mathcal{H}(\tau)-\mathcal{H}(\sigma)$.

The question remains of how to cool the system down and how to determine the start temperature T_s and the end temperature T_e. A universal method for determining T_s [3] is by performing an initial random walk at infinite temperature (i.e., all moves are accepted), measuring the occurring energy differences $\Delta\mathcal{H}$, and specifying the start temperature T_s of the simulation by

$$T_s=10\max\{\Delta\mathcal{H}\}. \tag{5}$$

The temperature is lowered logarithmically by

$$T_{\text{new}}=\alpha T_{\text{old}} \tag{6}$$

with a cooling factor α (usually $0.8\leqslant\alpha\leqslant0.999$) until the system freezes at a very low temperature.

This approach of finding at least a quasioptimum solution for a given problem by starting at a random configuration and cooling the system down can be transferred to economic problems [4]: the costs of a business problem, which have to be minimized, are identified with the energy function. The temperature is reduced to the role of a control parameter only. By lowering this parameter, the system is transferred from a random high-cost to a feasible low-cost solution.

*FAX: +49-941-943-3196.
Email address: johannes.bentner@physik.uni-regensburg.de

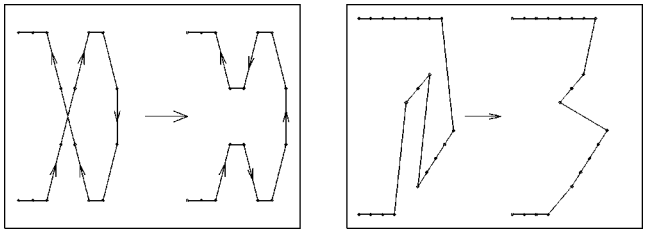

FIG. 1. Two simple moves that are often used: the Lin-2-Opt changes the direction of a part of the tour and the Lin-3-Opt exchanges two neighboring parts of the tour.

There are also some related algorithms, such as threshold accepting (TA) [5], which are based on the same annealing principle and which are widely used for solving problems from operations research like vehicle routing or production planning. They differ only in the exact choice of the transition probability function, which always depends upon a temperaturelike control parameter and the energies of the participating configurations. TA has been shown to provide results similar to SA, so we will only give results for SA throughout this paper.

B. Application to the traveling salesman problem

The traveling salesman problem (TSP) is given by a set of N cities or customers through which a traveling salesman has to find the shortest closed tour [6]. Every customer must be visited exactly once. All distances $D(i,j)$ between the customers are known to the traveling salesman. Therefore, the costs of the TSP are given by the length of the tour, i.e., by the sum over the lengths of the edges used. A configuration of the TSP is usually written as a permutation σ of the numbers $\{1,\ldots,N\}$, such that the Hamiltonian is given by

$$\mathcal{H}(\sigma)=D(\sigma(N),\sigma(1))+\sum_{i=1}^{N-1} D(\sigma(i),\sigma(i+1)). \quad (7)$$

(The first separate term is needed to close the tour.) The distances can be measured in units of either length or time, such that one can study a TSP that looks at minimal distance or at minimal travel time. If one faces a problem with a constant velocity that is exactly the same on all streets, then these two problems become equivalent.

There are many possibilities for creating a new configuration from the actual one. Mostly, only ''small'' moves are used, which do not change a configuration significantly. Due to the local effects of these moves, this principle is called local search: the algorithm tries to find an improvement in the neighborhood surrounding the actual configuration. This neighborhood structure combined with the set of all possible configurations results in the search space. Due to the local search principle, the energy landscape, which can be constructed by plotting the energy values over the search space, usually shows a relatively slightly curved valley-hill structure without many zigzags as the energies of neighboring configurations do not differ very much. For the TSP, it has been shown that using the Lin-2-Opt and the Lin-3-Opt moves, which are shown in Fig. 1, leads to the best results [7,8]: the Lin-2-Opt move simply reverses the direction of a part of the tour and the Lin-3-Opt move exchanges two successive parts of the tour without altering their directions.

When considering the TSP, there are also some thermodynamic observables that are interesting for optimization: first of all, the thermic expectation value of the energy $\langle\mathcal{H}\rangle$ shows how ''cheap'' the solutions at the given temperature already are. The specific heat C is given as the derivation of $\langle\mathcal{H}\rangle$ with respect to T and can therefore be written as

$$C=\frac{\mathrm{Var}(\mathcal{H})}{T^2}\equiv\frac{\langle\mathcal{H}^2\rangle-\langle\mathcal{H}\rangle^2}{T^2} \quad (8)$$

if the system is equilibrated. C indicates fluctuations in the system. The position of its peak is usually called the freezing temperature T_f of the system. At this temperature, the main part of the optimization has already been performed, so that the global patterns of the solution are already given. However, the system is still able to find many small improvements and therefore to optimize the problem locally.

The computational results for $\langle\mathcal{H}\rangle$ and C are shown in Fig. 2 for the specific instance BIER127; a problem consisting of the 127 beer gardens in the area of Augsburg, which can be found in Reinelt's library TSPLIB95 [9]. The left part of Fig. 2 shows how the mean energy decreases sigmoidally from the values of the completely random solutions to its optimum value. Consistent with this, the specific heat (on the right side) vanishes for $T\to\infty$ and $T\to 0$ and shows a peak at $T_f\approx 900$, which is relatively symmetric on a logarithmic T axis.

If the Hamiltonian consists of more than one energy contribution, e.g., $\mathcal{H}=\lambda_0\mathcal{H}_0+\lambda_1\mathcal{H}_1$, then a susceptibility χ_i can be defined for each of the $\mathcal{H}_i$ in order to measure the response of the system to the force that is exerted upon it by the ith term. The susceptibility is defined as

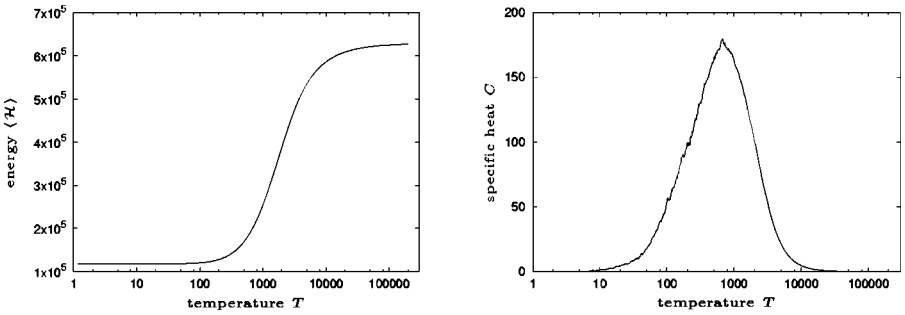

FIG. 2. Energy and specific heat of the normal TSP with SA algorithm for the problem of the 127 beer gardens in the area of Augsburg.

$$\chi_i = -\frac{\partial\langle\mathcal{H}_i\rangle}{\partial\lambda_i}. \tag{9}$$

(For example, think of the Zeeman term and the magnetic susceptibility being defined as the partial derivative of the magnetization with respect to the magnetic field.) In equilibrium, this susceptibility can also be written as

$$\chi_i = \frac{\mathrm{Var}(\mathcal{H}_i)}{T}. \tag{10}$$

II. THE TIME-DEPENDENT TRAVELING SALESMAN PROBLEM

The standard TSP is a relatively abstract problem: among many simplifications, the traveling salesman moves with the same velocity on a certain road at all times. The distance matrix or the travel time matrix $(D(i,j))$ is given as a constant. However, in reality, the time distance between two cities is not at all constant. There are many approaches to dealing with this problem: in a frequently used approach, the distance $D(i,j)$ between the cities i and j is dependent upon the position of the corresponding edge in the tour, i.e., a third dimension t is introduced in the distance matrix $D(i,j,t)$ [10,11] so that the distance between i and j is dependent upon the number of cities already visited in the tour. Therefore, the length of the tour is given by

$$\mathcal{H}(\sigma) = D(\sigma(N),\sigma(1),N) + \sum_{t=1}^{N-1} D(\sigma(t),\sigma(t+1),t). \tag{11}$$

This ansatz is usually called the *time-dependent* traveling salesman problem (TDTSP) and was introduced by Fox [12], who illustrated it with examples from the brewing industry. Note that the time index t does not mark the real time, but counts only the number of points visited regardless of the lengths of the distances between these points. However, in a real traffic scenario, the time distance between two cities is not dependent upon the previous part of the tour but on the time of day: in some regions, traffic jams occur at certain times.

Hence, on some streets the velocity of the traveling salesman is largely dependent upon the time. Due to the decreasing velocity, the time distances $D(i,j)$ between the cities are increased. Thus, the distance matrix that contains all distances $D(i,j)$ becomes time dependent. This more realistic problem, which is also referred to as the TDTSP in the literature [13], is an extension of the classical TSP and also nondeterministic polynomial (NP) complete [14]. NP complete means for practical purposes that there is no algorithm that is able to solve this problem in a computing time $t \propto N^p$, with N being the system size and p a polynomial expert.

In realistic problems, one of the most frequently seen situations is that of traffic jams occurring during rush hours, especially in the centers of large cities. Usually, the density of vehicles does not vary very much during these rush hours, so that we can introduce a constant factor f, which determines how the velocity decreases in contrast to freely moving traffic. According to another point of view we may also retain the velocity at its previous value, whereas the lengths of the streets are increased by this factor f. Usually, rush hours appear more frequently in the morning and in the evening. However, we wish to restrict ourselves to the special case in which traffic jams commence at a given time of day $\mathcal{M}$ and do not terminate until the traveling salesman arrives home. By using this scenario, we obtain similar results to those in the real case. However, we can show the effects of introducing rush hours into the TSP more precisely. In conclusion, we wish to study the following specific problem: We define a convex region in the city center in which traffic jams occur on all streets with the starting and the final points inside this region. Relating to this region we define an edge matrix η between the single customers with

$$\eta(i,j) = \begin{cases} 1 & \text{if both customers } i \text{ and } j \text{ are} \\ & \text{inside the traffic jam area.} \\ 0 & \text{otherwise .} \end{cases} \tag{12}$$

Therefore, the objective function can be written as

$$\mathcal{H}(\sigma) = \sum_{i=1}^{N} (D(\sigma(i),\sigma(i+1))\{1+\eta(\sigma(i),\sigma(i+1))(f-1) \times[\Theta(\zeta_{i-1}(\sigma))+C_i(\sigma)]\}), \tag{13}$$

with $D[\sigma(N),\sigma(N+1)] = D[\sigma(N),\sigma(1)]$ and

$$\zeta_i(\sigma) = \left(\sum_{j=1}^{i} D(\sigma(j),\sigma(j+1))\right) - \mathcal{M}, \tag{14}$$

which becomes greater than zero if the rush hour has already begun by the time the traveling salesman arrives at the customer i. The Heaviside function is defined by

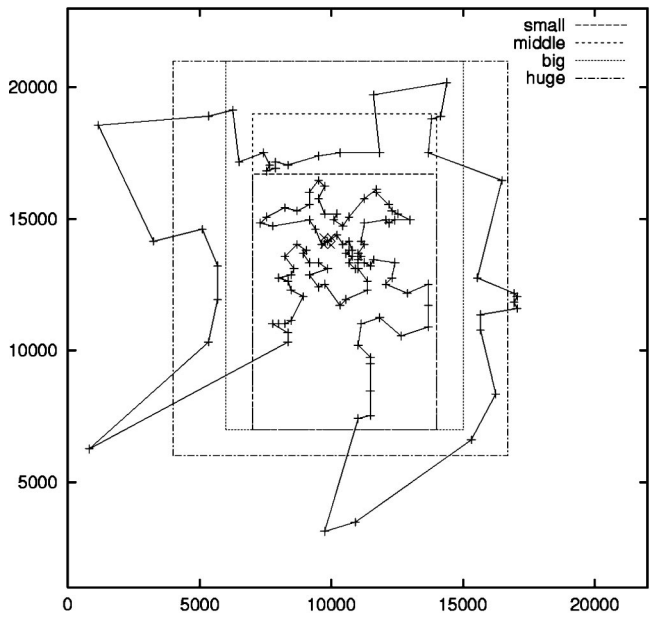

FIG. 3. The different traffic jam areas.

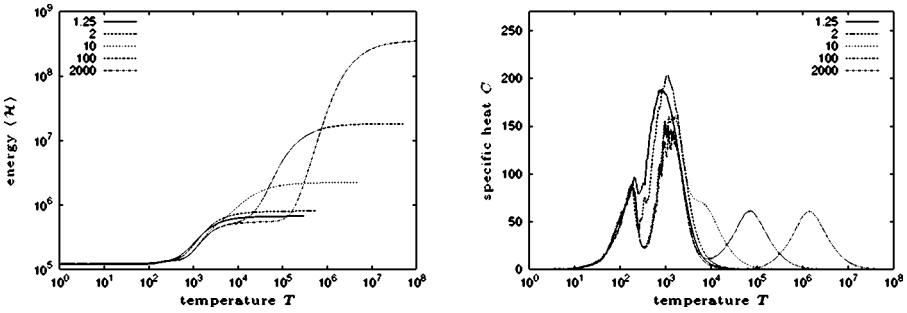

FIG. 4. Energy and corresponding specific heat in the small traffic jam area. Note that the single peak of the specific heat of the original benchmark problem splits into three peaks.

$$\Theta(x)=\begin{cases}1 & \text{if } x\geqslant 0\\ 0 & \text{otherwise.}\end{cases} \tag{15}$$

Equation (13) means that the time lengths of the streets the traveling salesman uses inside the city center are increased by the factor f after the beginning of the rush hour $\mathcal{M}$. [Therefore, $D(i,j)$ denotes the time the traveling salesman requires to travel from i to j if there is no traffic jam on this road.] The correction term

$$C_i(\sigma)=\Theta(\zeta_i(\sigma))[1-\Theta(\zeta_{i-1}(\sigma))]\frac{\zeta_i(\sigma)}{D(\sigma(i),\sigma(i+1))} \tag{16}$$

is needed to take into account the case in which the traveling salesman is using a road with $\eta=1$ when the rush hour commences. When this occurs, the traveling salesman can only drive slowly upon the remaining part of this road.

By considering this problem from another point of view, we could assume that instead of driving upon the roads in the traffic jam area after $\mathcal{M}$ at a slower velocity, the traveling salesman could drive upon these roads at the normal velocity $v=1$ but has to wait for a certain amount of time upon this road, so that the total time he spends here is equal to the required time for the road increased by the factor f. Therefore, we may rewrite the Hamiltonian $\mathcal{H}$ as

$$\mathcal{H}=\mathcal{H}_{\text{length}}+\mathcal{H}_{\text{time}} \tag{17}$$

with $\mathcal{H}_{\text{length}}$ being the actual tour length and $\mathcal{H}_{\text{time}}$ being the amount of time he needs due to the slowly moving traffic. Additionally, we may define the detour $\mathcal{H}_{\text{de}}$ by

$$\mathcal{H}_{\text{length}}=\mathcal{H}_{\text{de}}+\mathcal{H}_{\text{opt}} \tag{18}$$

with $\mathcal{H}_{\text{opt}}=118\,293.52$ being the optimum tour length for the original BIER127 problem and $\mathcal{H}_{\text{de}}$ being the distance of the detour that the traveling salesman has to drive because the system is not yet fully optimized and also because of avoiding the rush hour area after noon, so that we can write the Hamiltonian as

$$\mathcal{H}=\mathcal{H}_{\text{opt}}+\mathcal{H}_{\text{de}}+\mathcal{H}_{\text{time}}\ . \tag{19}$$

Because $\mathcal{H}_{\text{opt}}$ is a constant and $\mathcal{H}_{\text{de}}$ and $\mathcal{H}_{\text{time}}$ are competing parts in the Hamiltonian, it is very interesting to see how the algorithm balances between the two constraints (driving no detours and avoiding rush hours); this is dependent upon the traffic jam factor f.

In this paper, we intend to concentrate on self-made benchmark instances that are based on the BIER127 problem. We extended this BIER127 problem by adding a region of a certain size in the city center of Augsburg. The different regions and the nodes of the BIER127 problem are shown in Fig. 3. The traveling salesman is supposed to leave a depot (one of the original points in the BIER127 problem chosen by us) in the city center at 6 a.m. and return to the depot at 6 p.m. if no jams occur and if he uses the shortest possible tour, which has an optimum length of 118 293.52 (length given in REAL*8 metric). Therefore, one hour corresponds to a length of 118 293.52/12 due to his constant velocity v. The commencement of the rush hour $\mathcal{M}$ was set to noon (12 o'clock), which is equivalent to a time length of 118 293.52/2 = 59146.76. This would make it possible for the traveling salesman to drive without any restrictions until noon. After noon he should try to avoid roads that begin and end in the area defined above.

III. COMPUTATIONAL RESULTS

A. Comparison of different traffic jam factors

First of all, the effect of the traffic jam factor and therefore the traffic jam strength on the optimization has to be discussed. In order to do this, we initialized the problem with

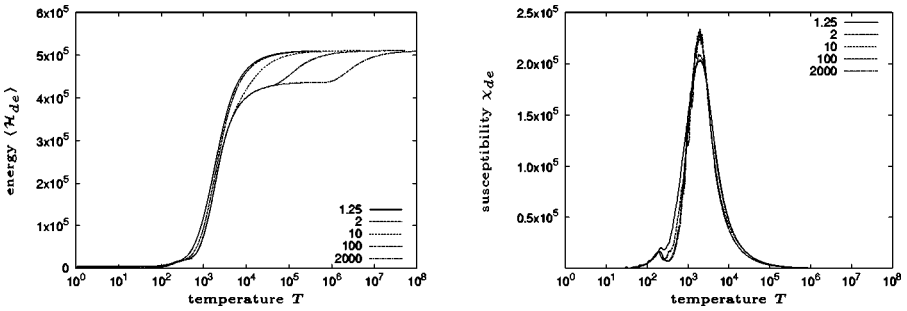

FIG. 5. The detour that the traveling salesman has to make in order to avoid the traffic jams and its corresponding susceptibility. For the larger traffic jam factors, the ordering and clustering effects can be seen.

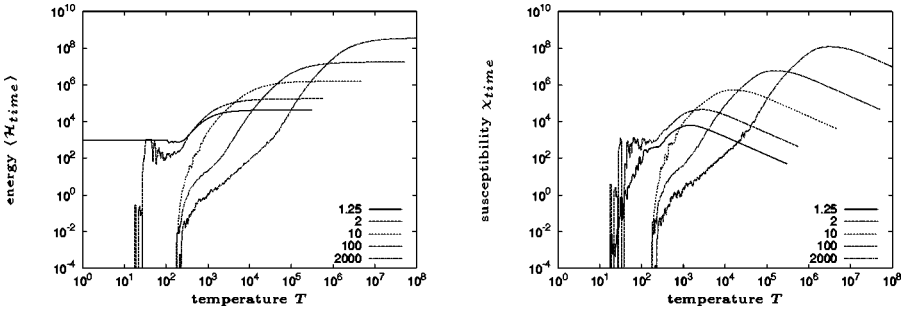

FIG. 6. Time that the traveling salesman spends in the traffic jam and corresponding susceptibility. The position of the susceptibility peak is linearly dependent upon the traffic jam factor.

the small traffic jam area and traffic jam factors $f=1.01$, 1.25, 1.3, 1.4, 1.5, 1.6, 1.75, 1.8, 2, 10, 50, 100, 200, and 2000. In the following, only the results for $f=1.25$, 2, 10, 100, and 2000 are listed because the results for these five factors demonstrate all significant changes within the optimization process. By choosing $f=1.01$, the original benchmark problem is hardly modified, whereas $f=2000$ means that the traffic comes to a halt after the daytime $\mathcal{M}$ in the city center.

By looking at Fig. 4, we can see at a glance that the start temperature increases with increasing *f*. This fact becomes quite clear if we consider that the energy differences in the random walk must be greater when *f* is increased. In fact, the start temperature T_s is linearly dependent upon *f* with a factor of $\approx 5.2\times 10^5$. At high temperatures, the system is in a random walk mode, i.e., it can move with virtually no restrictions through the energy landscape so that we obtain a flat curve for $\langle \mathcal{H} \rangle$ at high *T*. The height of this plateau is also linearly dependent upon *f*: $\langle \mathcal{H} \rangle_s \approx 1.8\times 10^5 f$. (The index *s* denotes the starting value at high temperatures.) On lowering the temperature, all curves decrease until the system freezes for $T \leqslant 10$. In contrast to Fig. 2, the decrease of $\langle \mathcal{H} \rangle$ is not exactly sigmoidal anymore: the mean energy shows a plateau at $T \approx 185$ already for small *f*. This leads to an incursion in the peak of the corresponding specific heat, which increases along with *f*. For large traffic jam factors *f*, we additionally find an extended plateau of the mean energy at medium temperatures ($T \approx 10\,000$). Therefore, depending upon the size of the traffic jam factor *f*, the optimization run can be split into up to three steps, as sketched in Fig. 4, and which can also be clearly seen in the specific heat, for which up to three peaks can be counted: the left two peaks are the remaining parts of the specific heat for $f=1$ (which is equal to the original problem without any rush hours), which is shown in Fig. 2. Comparing the positions of these peaks, we see that the left peak is far to the left of the original peak whereas the middle peak is shifted only slightly toward the right. On increasing *f*, a third peak grows from the right hand side of the middle peak of the specific heat, which migrates to higher temperatures linearly with increasing *f*. Moreover, the middle peak becomes lower with increasing *f*, because at lower *f* the right peak does not disappear but superposes on the middle peak.

By creating a movie of the actual routes at the different temperatures during the simulation, we were able to visualize the evolution from the random start configuration to the optimal tour. In this way we were able to verify that the right peak stems from an optimization process, by which the rough chronology of the tour is determined (ordering by time). This means that, at temperatures lower than the position of this peak, the traveling salesman visits the customers living in the city center in the forenoon, in order to avoid the traffic jam in the center that will occur in the afternoon. The left and the middle peaks simply result from an ordering and clustering process, which is also well known through other optimization problems like circuit layout [4,15]: due to the different length scales between the beer gardens inside the city center of Augsburg and the beer gardens in the villages near Augsburg, we first find a clustering in those areas where longer edges are to be found and subsequently (at lower *T*) an ordering process inside the city center, where the shorter edges are located.

These findings of three different transitions can be clearly verified by taking a look at the partial energies and their corresponding susceptibilities. Figure 5 shows the detour $\langle \mathcal{H}_{\rm de} \rangle$ and its susceptibility. Again, for small *f*, we find only two decreases of the energy: a larger one at a temperature of approximately 2000 and a relatively small one at a temperature of 200. For $f=100$ and $f=2000$ we find a third decrease: the mean partial energy decreases from the level at which the configurations of the random walk lie to an intermediate level, upon which a restricted random walk is possible. A restricted random walk means that the rough chronology of the tour is already determined. This third transition is not seen at all at the susceptibility $\chi_{\rm de}$. The susceptibility $\chi_{\rm de}$ shows a large peak at the critical temperature $T_{c,\rm de} \approx 2000$ and a small second peak at 200; the temperatures at which the peaks lie are not dependent upon the size of *f*. However, the exact height of the peak is not fully dependent upon the size of *f*: using values of $f<10$, one can find heights of between 203 000 and 210 000; working with

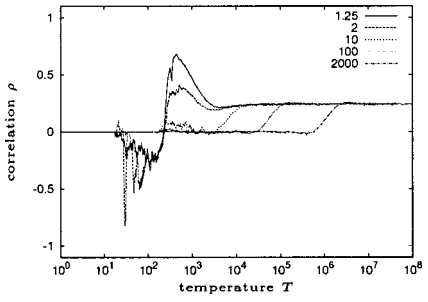

FIG. 7. The correlation between the lost time and the detour. The starting correlation is equal for all traffic jam factors. The higher the factor, the earlier the correlation disappears. An anticorrelation can be measured for small factors only.

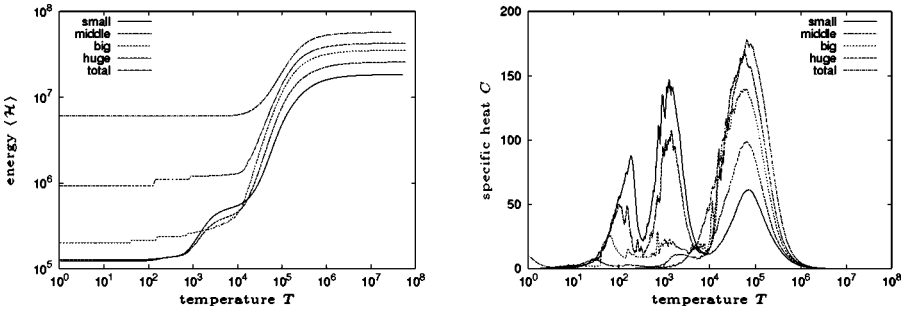

FIG. 8. Energy and corresponding specific heat in a traffic jam problem of size $f=100$ in a comparison of the five different traffic jam areas.

$f \geqslant 10$, one obtains peak heights of between 225 000 and 235 000.

Due to the different orders of magnitude in the results for $\langle \mathcal{H}_{\text{time}} \rangle$ and its corresponding susceptibility χ_{time}, we had to plot the results double-logarithmically in Fig. 6. By viewing the left part of Fig. 6, we discover that the starting value of $\langle \mathcal{H}_{\text{time}} \rangle$ is strongly dependent upon f in contrast to $\langle \mathcal{H}_{\text{de}} \rangle$, which was exactly constant. Similarly to $\langle \mathcal{H} \rangle_s$, $\langle \mathcal{H}_{\text{time}} \rangle_s = 1.8 \times 10^5 f$ for large f. For $T \to 0$, a small waiting time remains if $f=1.25$ because, in this case, a detour would take more time than this waiting period in the traffic jam. In contrast to this, the traveling salesman has to avoid the traffic jam area for higher values of f. Unlike the peaks of the detour susceptibility in Fig. 5, which result from ordering and clustering and do not fully depend upon f, the peak positions of the time susceptibility are shifted toward higher temperatures linearly by a factor of 1.7×10^3 with f. The positions of the peaks of χ_{de} and χ_{time} are identical for $f=1.5$ and the peak of χ_{time} is to the right of the peak of χ_{de} for $f>1.5$. For small f up to $f=2$, there is a large overlap between the peaks of χ_{time} and χ_{de}, i.e. the optimization process tries to fulfill both constraints (making no detours and wasting no time in traffic jams) simultaneously. For $f \geqslant 10$, the overlap vanishes: the system is ordered first according to the time constraint and then according to the detours. The heights of the peaks of χ_{time} also depend upon f; they increase as $6 \times 10^4 f$ for large f.

The linear dependencies of the peak position $T_{c,\text{time}}$ and $\langle \mathcal{H}_{\text{time}} \rangle_s$ appear quite clear due to the linear influence of f in the Hamiltonian. Small variations within the linear behavior can be observed only for small f and result from the finite system size. Since f can be seen as a simple scaling factor, the curves for $\langle \mathcal{H}_{\text{time}} \rangle$ and χ_{time} coincide for large f if we use parametric sizes T/f and χ_{time}/f that do not depend upon f.

Finally, we should look at the correlation between $\langle \mathcal{H}_{\text{de}} \rangle$ and $\langle \mathcal{H}_{\text{time}} \rangle$ during the optimization run. The results are shown in Fig. 7. Independently of f, all curves start at the same value of ≈ 0.24. Therefore, we have a basic correlation between the constraints of driving no detour and avoiding traffic jams in the system. This fact becomes quite clear if we consider that for random solutions an improvement in the tour length also shortens the time for which the traveling salesman has to wait. For smaller T, the curves for the various f show varied behavior: for small f, we first see a peak of ρ in almost the same temperature range in which the breakdown of the middle peak of the specific heat occurs. After that, for smaller T, the partial energies are anticorrelated. In this temperature range, the two conditions work against each other if the system tries to fulfill both constraints simultaneously. This behavior is not seen for larger f; there, the correlation simply vanishes at high temperatures. Obviously, for large f, the optimization is performed separately for the two constraints: First, the traveling salesman has to avoid the rush hour area after noon. When the system is caught in a valley of the energy landscape, with all states in this valley fulfilling this condition $[\langle \mathcal{H}_{\text{time}} \rangle \equiv \text{const} \Rightarrow \rho \to 0]$, then the optimization due to the tour length is started. This result coincides with the discussion of the overlaps of the susceptibilities and with the graphics in Fig. 5, in which the partial energy for the detour breaks down to a lower value and remains nearly constant throughout a large temperature interval.

B. Comparison of different traffic jam areas

In contrast to the last subsection, in which we discussed the influence of the size of the traffic jam factor f on the system, we now intend to study how the results are affected if the traffic jam area is either extended or minimized. Here we wish to discuss results for the different traffic jam areas shown in Fig. 3, by using a traffic jam factor $f=100$. We decided on this large factor because we wished to see the

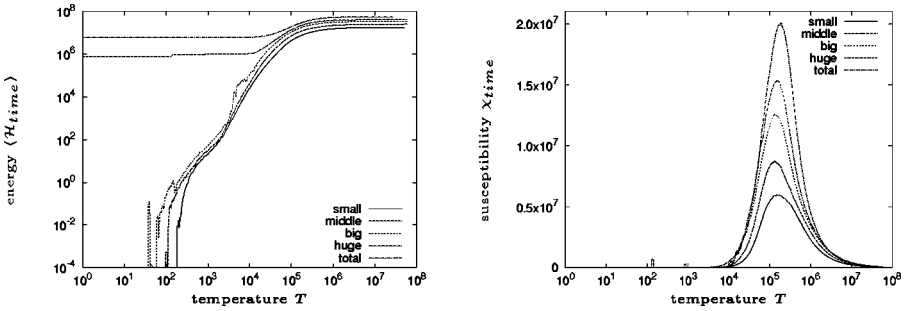

FIG. 9. The time the traveling salesman has to spend in the traffic jam and the corresponding susceptibility. The heights of the susceptibility peaks vary at the fourth power with the size of the traffic jam area.

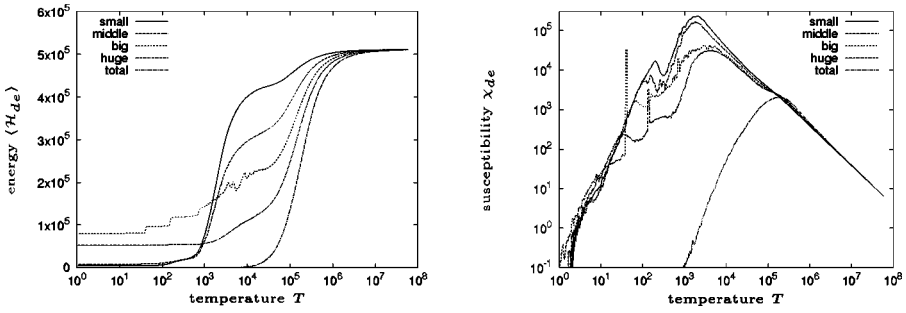

FIG. 10. The detour the traveling salesman has to take into account in the different configurations and its corresponding susceptibility. Notice that the detour first increases with increasing size of the traffic jam zone and then decreases again.

effects on the different optimization steps separately. The total traffic jam zone contains all cities: the huge 118, the big 107, the middle 102, and the small 91. The number of cities inside this traffic jam zone will be denoted as N_j throughout this section. We will show that some observables have an N_j^4 dependency in contrast to the previous section, in which the dependency was linear with to f.

The system energy, which can be seen in Fig. 8, shows no intermediate plateau for the total and the huge traffic jam areas. This indicates that there is only one constraint that dominates the system in the case of large N_j. Due to the large size of the traffic jam region, there is no longer an ordering and clustering effect. If the area is decreased then the intermediate plateau due to the ordering and clustering effect reappears. This behavior can be verified by the specific heat, which displays only the right time ordering peak for the two largest zones. The height of this peak is roughly given by $8\times10^{-7}N_j^4$ and is therefore strongly dependent upon the number of cities in the traffic jam area.

Looking at the starting values of the mean energy (Fig. 8) and of the partial energy for the waiting time (Fig. 9), $\langle \mathcal{H} \rangle_s$ and $\langle \mathcal{H}_{\text{time}} \rangle_s$, we find that they are given by $\approx 0.24 N_j^4$. This behavior can be explained simply if we consider that N_j increases quadratically with the linear extension of the traffic jam area and that there are $\mathcal{O}(N_j^2)$ connections between the N_j cities. The linear dimension of the traffic jam area is an indirect measure of the lengths of these connections, so that we get an $\mathcal{O}(N_j^4)$ behavior all in all. (Of course, this argument is exact only for a large system of randomly distributed cities. We cross checked our assumption with the results for a few randomly generated TSP examples, for which we again found the N_j^4 dependencies, which are described here for the BIER127 instance.) On the other hand, the size of $\langle \mathcal{H}_{\text{de}} \rangle_s$ is not affected significantly by the value of N_j, as can be clearly seen in Fig. 10.

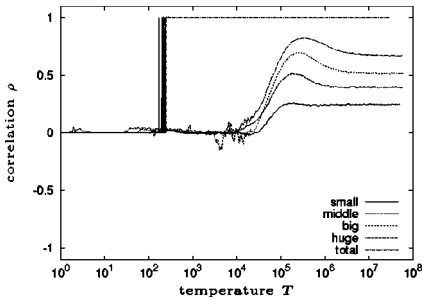

FIG. 11. The correlations between the time and the detour. The starting values of the correlation are dependent upon the system configuration.

Considering the corresponding susceptibilities, we find that the height of the peak of χ_{de} in Fig. 10 decreases with increasing N_j. Furthermore, the peak is shifted to higher values of T (with an exception between the small and middle zones); however, here we cannot give any quantitative dependencies. In particular, we find that the curve for the total zone is completely separated from the other curves. The other curves show many additional fluctuations and small peaks on the left leg of the susceptibility, which might be explained by the geometric positions of the single beer gardens. By looking at Fig. 9, we find that the peak of χ_{time} is always sited at roughly the same temperature ($T = 188\,164.498$ for the total zone, for which the peaks of χ_{de} and χ_{time} are at the same temperature). The height of the peak is roughly given by $\approx 0.08 N_j^4$, so that we again obtain this dependency on the fourth order of N_j.

If the traffic jam areas are small, the traveling salesman has enough choices by which to avoid the traffic jams by bypassing the city center without impairing his costs too greatly. By increasing the size of the traffic jam area, it becomes more and more unavoidable for the traveling salesman to take a short detour, which, however, is much cheaper in this situation ($f = 100$) than waiting in the traffic jams. If the traffic jam zone contains nearly all or all cities then the traveling salesman no longer has the option to escape the traffic jams. In conclusion, an impairment of the total energy results for the three smaller zones in a driven detour and for the huge and total zones in the waiting time. This can be verified in the remaining part of the detour, which is plotted in Fig. 10 and the remaining part of the time, which is plotted in Fig. 9. Notice that the remaining detour decreases again for the huge and total zones, because in these cases there are not enough possibilities for driving a detour, as there are only 9 (0) cities left in the suburb. In contrast to this, the waiting time in the cases for these two zones is much larger than for the smaller ones.

Finally, we wish to have a look at the correlation between $\langle \mathcal{H}_{\text{de}} \rangle$ and $\langle \mathcal{H}_{\text{time}} \rangle$ which is plotted in Fig. 11. In contrast to the results shown in Fig. 7, the start values $\langle \rho \rangle_{s,j}$ of the correlation vary at high temperatures, due to the five different configurations of the traffic jam problem. The dependency of these start values upon the number of cities in the traffic jam area N_j is again proportional to the fourth power of N_j. The same dependency is valid for the peak heights. The reasons are the same as mentioned above for $\langle \mathcal{H} \rangle_s$,

$\langle \mathcal{H}_{\text{time}} \rangle_s$, and the peak height of χ_{time}. The correlation for the total zone forms an exception: driving a detour does not help to minimize the waiting time in the traffic jams, because no road is free of traffic jams. In this way both constraints can be optimized at the same time. They are completely correlated ($\rho = +1$) at high temperatures. When freezing effects take place, the detour and the waiting time cannot continue to fluctuate. In this case, the correlation between the two physical values is not defined because zero is divided by zero. In this temperature range we set the correlation to zero.

IV. CONCLUSION

In our paper, we studied the time-dependent traveling salesman problem as defined by us, by introducing a zone in the city center in which traffic jams occur in the afternoon. We gave a detailed derivation of the Hamiltonian $\mathcal{H}$ of this problem and showed how $\mathcal{H}$ can be split into two different parts, each of them addressing one of the two constraints in this problem: driving no detour and spending no time in a traffic jam. We managed to show how the simulated annealing and threshold accepting algorithms are able to handle such time-dependent problems. Applied to a benchmark problem based on the BIER127 problem with different traffic jam areas, we were able to observe how the two constraints of detour and waiting time work against each other and the system finally reaches an optimum.

ACKNOWLEDGMENTS

We wish to thank Heidi Scarlett (University of Regensburg, Germany), Erich Stoll (University of Zurich, Switzerland), and Sigismund Kobe (Technical University of Dresden, Germany) for fruitful discussions. Part of the work was financed by the Swiss National Science Foundation.

[1] K. Binder and D. W. Heermann, *Monte Carlo Simulation in Statistical Physics* (Springer, Berlin, 1992).
[2] N. Metropolis, A. W. Rosenbluth, M. N. Rosenbluth, A. H. Teller, and E. Teller, J. Chem. Phys. **21**, 1087 (1953).
[3] T. Scheuer (private communication).
[4] S. Kirkpatrick, C. D. Gelatt, Jr., and M. P. Vecchi, Science **220**, 671 (1983).
[5] G. Dueck and T. Scheuer, J. Comput. Phys. **90**, 161 (1990).
[6] G. Reinelt, *The Traveling Salesman* (Springer, Berlin, 1994).
[7] P. F. Stadler and W. Schnabl, Physica D **48**, 65 (1991).
[8] S. Kirkpatrick and G. Toulouse, J. Phys. (Paris) **46**, 1277 (1985).
[9] G. Reinelt, computer code TSPLIB95 (Universität Heidelberg, Germany, 1995), http://www.iwr.uniheidelberg.de/iwr/comopt/software/TSPLIB95
[10] C. Bastian and A. H. G. Rinnooy Kan, Eur. J.Oper. Res. **56**, 407 (1992).
[11] R. J. Vander Wiel and N. V. Sahinidis, Nav. Res. Logist. **43**, 797 (1996); Transp. Sci. **29**, 167 (1995).
[12] K. R. Fox, PhD thesis, John Hopkins University, 1973.
[13] C. Malandraki and M. S. Daskin, Transp. Sci. **26**, 185 (1992).
[14] C. Malandraki and R. B. Dial, Eur. J. Oper. Res. **90**, 45 (1996).
[15] I. Morgenstern, in *Heidelberg Colloquium on Glassy Dynamics*, edited by L. van Hemmen and I. Morgenstern (Springer, Heidelberg, 1986), pp. 398–427.